AMSE JOURNALS-AMSE IIETA publication-2017-Series: Advances B; Vol. 60; N°2; pp 505-524
Submitted Apr. 08, 2017; Revised Jun. 12, 2017; Accepted Jun. 18, 2017

Study on Damage Identification of Beam Bridge Based on Characteristic Curvature and Improved Wavelet Threshold De-Noising Algorithm

Xi Chu*, Zhixiang Zhou, Guojun Deng, Tengjiao Jiang, Yangkun Lei

Dept. of State Key Laboratory Breeding Base of Mountain Bridge Tunnel Engineering, Chongqing Jiaotong University, Chongqing 400074, China (jfnchuxi@yahoo.com)

Abstract

With the point cloud data of box girder obtained by the theory of structure from motion (SFM) algorithm chosen as the research background, a damage identification method based on characteristic curvature and improved wavelet threshold de-noising algorithm is presented. Firstly, the static load test is carried out for the full-scale box girder model, and after the cracking damage, the discrete point cloud data on the surface of the box girder are obtained through the SFM theory. According to the basic hypothesis, deformation is mainly caused by the bending moment, and micro damage has no effect on stress redistribution. Therefore, a conclusion can be made that the curvature is sensitive to the structural damage. Then, a characteristic curvature damage identification method, which is based on point cloud chord length, is used to solve the characteristic curvature of the specified section of the box girder. It is found that there are a large number of point cloud noise signals in the characteristic curvature, and on this basis, a new wavelet de-noising method established upon the threshold function is proposed. Finally, the damage index revealed from the characteristic curvature after de-noising in the specified section is compared with the actual damage location of the box girder. The results show that by combining the characteristic curvature algorithm based on the chord length of scattered point cloud with the improved wavelet threshold de-noising function, the structural surface crack damage based on spatial point cloud data can be identified. Especially, in consideration of noise interference, the improved wavelet threshold de-noising function proposed in this paper can effectively suppress the high frequency noise signal in the characteristic curvature and preserve the low-frequency signal of damage in the damage area. Thus, the accuracy and sensitivity of the

damage identification method based on the characteristic curvature are guaranteed. This method has the potential to be applied to structural health monitoring, since it can provide a new technical method for the early warning of the beam structure bridge.

Key words

Damage identification, Feature curvature, SFM, Threshold function, Wavelet de-noising.

1. Introduction

As a new technique in the reverse engineering field, structure from motion (SFM) [1-4] algorithm means obtaining the multi view image set with motion camera and then estimating the pose of the camera and reconstructing the scene structure. The technique can generate high resolution 3D spatial data by taking a set of photographs covering the measurement area only. Through this unique data acquisition method, the 3D spatial data of the research object can be efficiently obtained in a non-contact way. At present, the technology has been adopted in the field of terrain reconstruction, regional measurement, vegetation statistics, digital terrain model building and so on [5-9].

Nevertheless, most of the researches focus on its application to the reconstruction of large scale terrain and the measurement of remote terrain, while there are some technical bottlenecks in the field of structural surface crack identification. These bottlenecks are mainly reflected in SFM in that the method needs to be optimized by bundle adjustment (BA) [10] method. That is to say, the three dimensional reconstruction of unstructured image can be successfully completed by the bundle adjustment method. However, when the 3D coordinates of the image are restored, the re-projection error of the spatial three-dimensional coordinates of the back calculation caused by the cumulative error of BA method is very uneven. As a result, the 3D reconstruction model will inevitably contain a large number of high frequency noises, the distribution of which makes it difficult for the topological reconstruction surface by point cloud to accurately reflect the position information of the structure crack [11]. In recent years, with the development of threshold wavelet mathematical theory, structural damage identification techniques based on point cloud data have been widely discussed. To a certain extent, the stable and efficient wavelet threshold de-noising algorithm can suppress the random noise in the process of point cloud formation [12-14], recognizing and preserving the original low frequency signal and the non noise high frequency signal well. In this way, a new way is provided for the damage identification of structural surface crack based on point cloud data. This paper is based on the basic hypothesis

that deformation is mainly caused by the bending moment and micro damage has no effect on stress redistribution. Moreover, it is proved that the curvature is sensitive to the damage location, and a method to estimate the characteristic curvature of discrete point clouds is also presented in this paper. For the problem that the original signal in the characteristic curvature is seriously disturbed by the point cloud noise, a new wavelet de-noising algorithm based on threshold function is proposed. The method can better identify the original low frequency signal and suppress the abnormal high frequency signal. Finally, the accuracy and sensitivity of the proposed damage identification method based on the characteristic curvature and the improved wavelet threshold de-noising function are verified by full-scale model test.

2. The Establishment of Digital Three-Dimensional Model for the Box Girder Damage Model

2.1 The Basic Principle of Sfm Algorithm

In recent years, a new type of digital photogrammetry technology called SFM has become an effective method for acquiring 3D data with low cost and high efficiency. In this method, an efficient feature matching algorithm is employed to automatically extract the 3D digital model of the object and the motion parameters of the camera from multi view images. For purpose of determining the three-dimensional coordinates of spatial objects, the traditional photogrammetric methods require that the orientation of the camera and the spatial coordinates of a series of control points should be known, because they need to determine the position of the control points in the image by artificial methods and then use the "resection" to determine the camera position. However, the SFM method is different from the traditional photogrammetry in that above conditions are not required to be known for scene reconstruction. Furthermore, this method is based on the feature matching data between images, and the azimuth of the camera along with the geometry of the scene can be automatically solved by the process of bundle adjustment (BA) [15]. The implementation of SFM method has benefited from the development of efficient automatic feature matching algorithm, and it is very suitable for reconstructing a digital 3D model by using a set of images with high overlap and changeable visual angle.

In SFM, each image corresponding to the camera is determined by 7 parameters, including 6 external parameters of rotation matrix R and translation vector T as well as one camera internal parameter f. In the process of scene reconstruction, the image with the maximum matching points should be selected as much as possible according to the principle of minimizing the re-projection error, and these images will be used as the initial constraint condition. With the continuous

increase of the images, the corresponding feature points are connected to form the feature point tracking trajectory, which is also known as the channel set. Then the channel set is utilized to restore the camera parameters and the camera's three-dimensional position information. The next step is to optimize the reconstructed camera and scene parameters with the iterative bundle adjustment method [16], which refers to using incremental ways to add a camera each time and optimize the parameters. With regard to the new camera, it needs to be able to see most of the three-dimensional scenes that have been reconstructed. Afterwards, DLT [17] (Direct Linear Transformation) algorithm is employed to restore the parameters of the new camera, and then the new camera recovery points are added into the optimization process. Subsequently, the bundle adjustment method is taken to optimize all of the 3D field spots and camera parameters that have been reconstructed. This process will be repeated, until all images are added. Finally, the 3D model is reconstructed from the image search strategy [18].

2.2 The Three Dimensional Reconstruction Model of Full Scale Box Girder Based on SFM Algorithm

The camera is used to shoot the box beam in multi angles, and 79 images of the box beam are taken. Part of the box beam images are given in figure 1.

Fig.1. Image Sequence of Indoor Box Beam Specimen

By using above SFM 3D point cloud reconstruction algorithm, the three dimensional reconstruction of the box girder specimen is carried out on the MATLAB platform. The results of the 3D reconstruction are illustrated in figure 2.

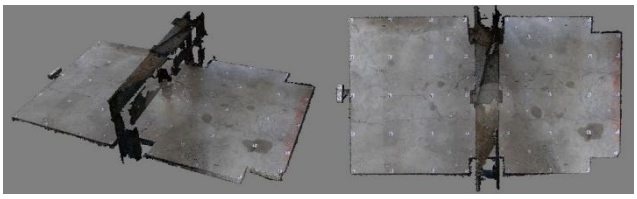

Fig.2. Three Dimensional Point Cloud Reconstruction Effect of Box Girder Specimen

When the 3D coordinates of the image feature point are restored, the accumulated error in the iterative bundle adjustment process is produced, which will lead to a very non-uniform projection error of the three dimensional coordinates and make the 3D coordinates of the point of the re-projection error in the back calculation process quite uneven. Thus, the 3D reconstruction model will inevitably contain a large number of high frequency noises. For the point cloud data of the box girder in this paper, the details of the effect of the spatial discrete point cloud can be seen in figure 3. After the amplification, it can be seen that there are many free points on the surface of the jack. According to Figure 4, the points distribute uniformly on both sides of a surface, forming the main body of the point cloud data. Under the joint action of the iteration error and the drastic change of the surface reflectivity, the point cloud data contains a large number of free points, and the hat is the noise points. These noise points reflect the outlier characteristics of the main point cloud, and the outlier noise points give rise to the measurement error, thereby making the generated 3D model surface deviate from the actual surface. In consequence, great interference is brought to the later surface modeling and the analysis of the crack on the surface of the box girder.

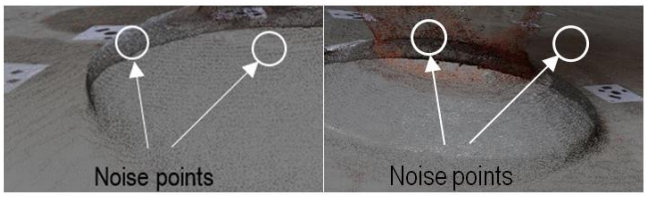

Fig.3. Details of the Effect of Spatial Discrete Point Cloud

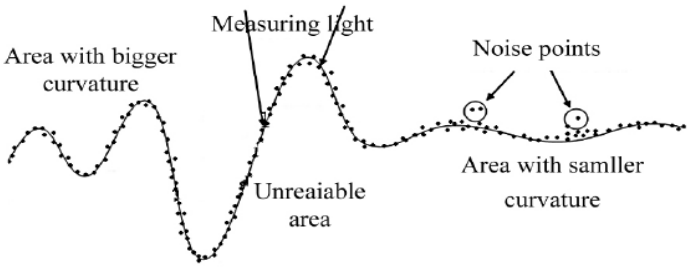

Fig.4. Distribution Characteristics of Outlier Noise Points

In addition, the 3D reconstruction point cloud data based on SFM algorithm has its own modeling error. Assuming that the surface in Figure 5 is the surface of the object and the real point is the intersection between the surface and line of the measuring point and the origin point. Taking point A as an example, the possible position of each measurement point of the camera in this direction is presented in the frequency histogram of fig 5. Moreover, the desired position of point A is point A', and the variance distance is σ2 A. When the least square method is used to estimate the parameters, it does not have the validity and consistency despite of its unbiasedness, which will reduce the accuracy of the three-dimensional model.

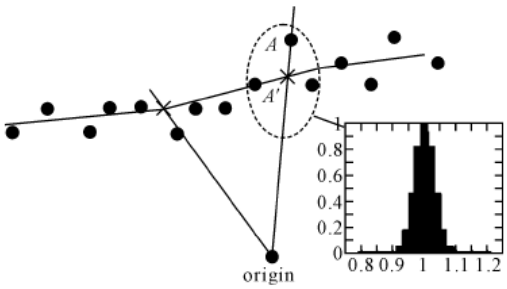

Fig.5. Sketch Map of Point Cloud Distribution

3. The Damage Identification Method Based on Characteristic Curvature

3.1 Correlation Analysis of Curvature and Crack Damage

According to the principle of virtual work in structural mechanics, the deflection of any point in the deformation structure is as follows:

$$y = \frac{1}{EI}\int M_i(x)M_F(x)ds + \frac{1}{EA}\int N_i(x)N_F(x)ds + \frac{1}{GA}\int \mu Q_i(x)Q_F(x)ds \tag{1}$$

For bridge structures, such as simple-supported beam, continuous beam as well as rigid frame bridge, the deflection is mainly caused by bending, and the shear deformation and axial deformation are very small. Therefore, the deformation value generated by shear force and axial force can be ignored, and formula 1 can be simplified as:

$$y = \frac{1}{EI}\int M_i(x)M_F(x)ds \tag{2}$$

At the same time, the curvature expression of the deflection curve is provided in formula 3 according to the higher mathematics:

$$\frac{1}{\rho(x)} = \pm \frac{y''}{\left[1+(y')^2\right]^{\frac{3}{2}}} \tag{3}$$

Among which $\rho(x)$ is the radius of curvature, and y is the deflection. Ignoring the higher order terms in formula 9, the approximate formula for the curvature of the deflection curve is as follows:

$$\frac{1}{\rho(x)} = y'' \tag{4}$$

The relationship between the bending moment and the deflection at any cross section can be got by material mechanics, as shown in equation 5:

$$EI\frac{1}{\rho(x)} = -M(x) \tag{5}$$

In which E is the elastic modulus, I is the moment of inertia, and $M(x)$ is the moment produced by the load. By importing formula 4 into formula 5, the relationship between the bending moment and the stiffness and deflection of any section of the beam is acquired as follows:

$$y'' = -\frac{M(x)}{EI} \tag{6}$$

When the form of the structure and the external load are constant, the deflection and the deflection curvature of any section are positively correlated with the section stiffness of the beam. When structural damage occurs in the beam, different degrees of stiffness degradation will take place in the beam at the location of the disease. At the same time, a sudden change will emerge in the deflection and deflection curvature. In other words, the curvature is sensitive to the location of damage. Based on this principle, the method of solving the characteristic curvature based on discrete point cloud is studied in this paper.

3.2 The Calculation Method of Discrete Point Cloud Feature Curvature Based on Chord Length

The parameter equation, in which the arc length is s, is adopted to represent the continuous graph outline curve:

$$\begin{cases} x = x(s) \\ y = y(s) \end{cases} \tag{7}$$

Then, the first derivative of x=x(s) and y=y(s) at point Z can be expressed as:

$$\begin{aligned} x'(s_0) &= \lim_{\Delta s \to 0} \frac{x(s_0 + \Delta s) - x(s_0 - \Delta s)}{2\Delta s} \\ y'(s_0) &= \lim_{\Delta s \to 0} \frac{y(s_0 + \Delta s) - y(s_0 - \Delta s)}{2\Delta s} \end{aligned} \tag{8}$$

The second derivative of x=x(s) and y=y(s) at point s_0 can be expressed as:

$$\begin{aligned} x''(s_0) &= \lim_{\Delta s \to 0} \frac{x'(s_0 + \Delta s) - x'(s_0 - \Delta s)}{2\Delta s} = \lim_{\Delta s \to 0} \frac{{}^{f}x' - {}^{b}x'}{2\Delta s} \\ y''(s_0) &= \lim_{\Delta s \to 0} \frac{y'(s_0 + \Delta s) - y'(s_0 - \Delta s)}{2\Delta s} = \lim_{\Delta s \to 0} \frac{{}^{f}y' - {}^{b}y'}{2\Delta s} \end{aligned} \tag{9}$$

Where

$$\begin{aligned} {}^{f}x' &= \lim_{\Delta s \to 0} \frac{x(s_0 + \Delta s) - x(s_0)}{\Delta s} \\ {}^{b}x' &= \lim_{\Delta s \to 0} \frac{x(s_0) - x(s_0 - \Delta s)}{\Delta s} \\ {}^{f}y' &= \lim_{\Delta s \to 0} \frac{y(s_0 + \Delta s) - y(s_0)}{\Delta s} \\ {}^{b}y' &= \lim_{\Delta s \to 0} \frac{y(s_0) - y(s_0 - \Delta s)}{\Delta s} \end{aligned} \tag{10}$$

Then the curvature at point x is:

$$C(s_0) = \frac{x'(s_0)y''(s_0) - x''(s_0)y'(s_0)}{[(x'(s_0))^2 + (y'(s_0))^2]^{3/2}} \tag{11}$$

For the curves of the discrete points that do not have analytical expressions, the curves can be expressed as a set of mutually inconsistent ordered points $Q_i(x_i,y_i)$, i=0, 1, …, n. L_i is set as the length of the line segment from point Q_{i-1} to Q_{i+1}; and M_i denotes the length of the line segment from point Q_{i-1} to Q_{i+1}, as presented in Figure 6.

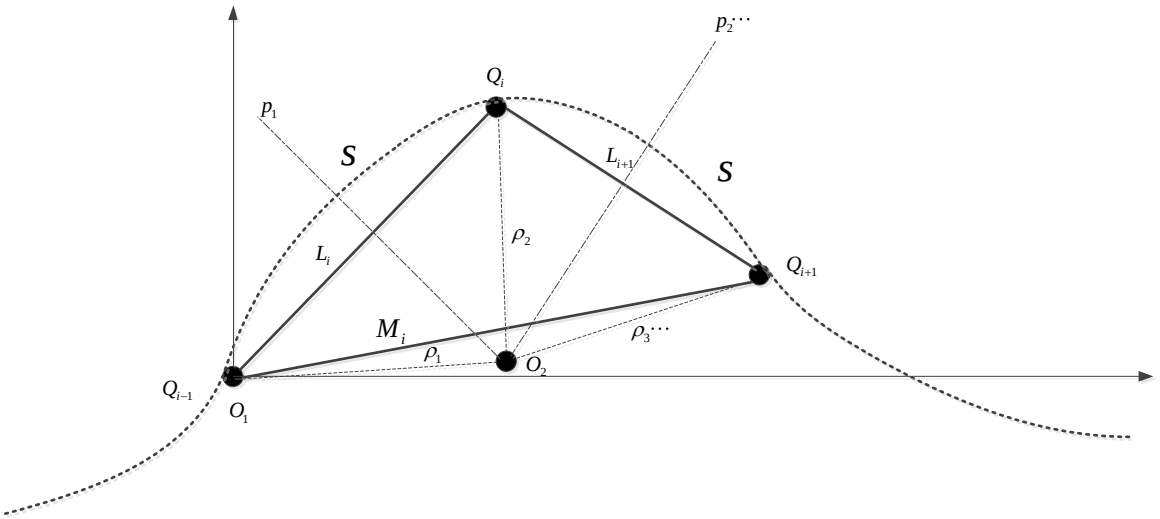

Fig.6. Curvature Calculation Model of Discrete Points

In order to approximately calculate the value of curvature at the discrete point Q_i, above formula for calculating the curvature of the continuous curve can be transformed, and the formula for calculating the curvature of the discrete point of the graphics outline is obtained. By sequentially connecting the discrete points, the outline of the graph is changed into a fold line. Furthermore, the length of the chord can be used to approximately represent the length of the arc. Then the first derivative of the discrete point Q_i can be expressed as:

$$x_i' = \frac{x_{i+1} - x_{i-1}}{L_i + L_{i+1}}; y_i' = \frac{y_{i+1} - y_{i-1}}{L_i + L_{i+1}} \tag{12}$$

The second derivative can be expressed as:

$$x_i'' = \frac{x_i'^f - x_i'^b}{L_i + L_{i+1}}; y_i'' = \frac{y_i'^f - y_i'^b}{L_i + L_{i+1}} \tag{13}$$

In which,

$$x_i^{'f} = \frac{x_{i+1} - x_i}{L_{i+1}}; x_i^{'b} = \frac{x_i - x_{i-1}}{L_i}$$
$$y_i^{'f} = \frac{y_{i+1} - y_i}{L_{i+1}}; y_i^{'b} = \frac{y_i - y_{i-1}}{L_i} \quad (14)$$

The formula of curvature can be expressed as:

$$C_i = \frac{x_i' y_i'' - x_i'' y_i'}{((x_i)'^2 + (y_i)'^2)^{3/2}} \quad (15)$$

After processing the above analytical equation, the discrete point curvature C_i at point Q_i can be obtained:

$$C_i = \frac{2(L_i + L_{i+1})^2 D_{Q_{i-1}Q_iQ_{i+1}}}{L_i L_{i+1} M^3} \quad (16)$$

Where is a directed area of triangular.

$$D_{Q_{i-1}Q_iQ_{i+1}} = \frac{1}{2}\sum_{j=i-1}^{i+1}(x_j y_{j+1} - x_{j+!} y_j) \quad (17)$$

The point cloud data of the surface damaged box girder are analyzed with three sections and the slice position is shown in figure 7. The point cloud data of cross sections 1-3 are also extracted, the distribution of which is displayed in Figure 8.

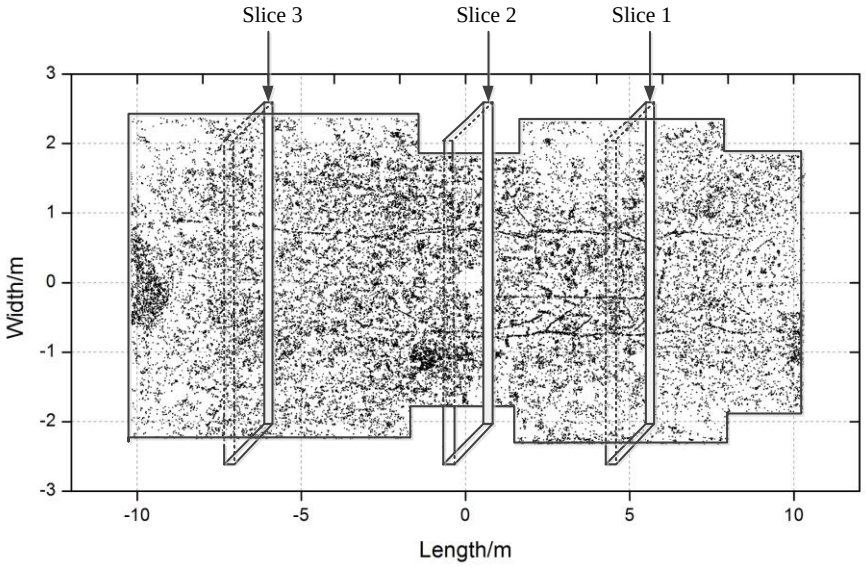

Fig.7. Slice Position of Box Girder Surface

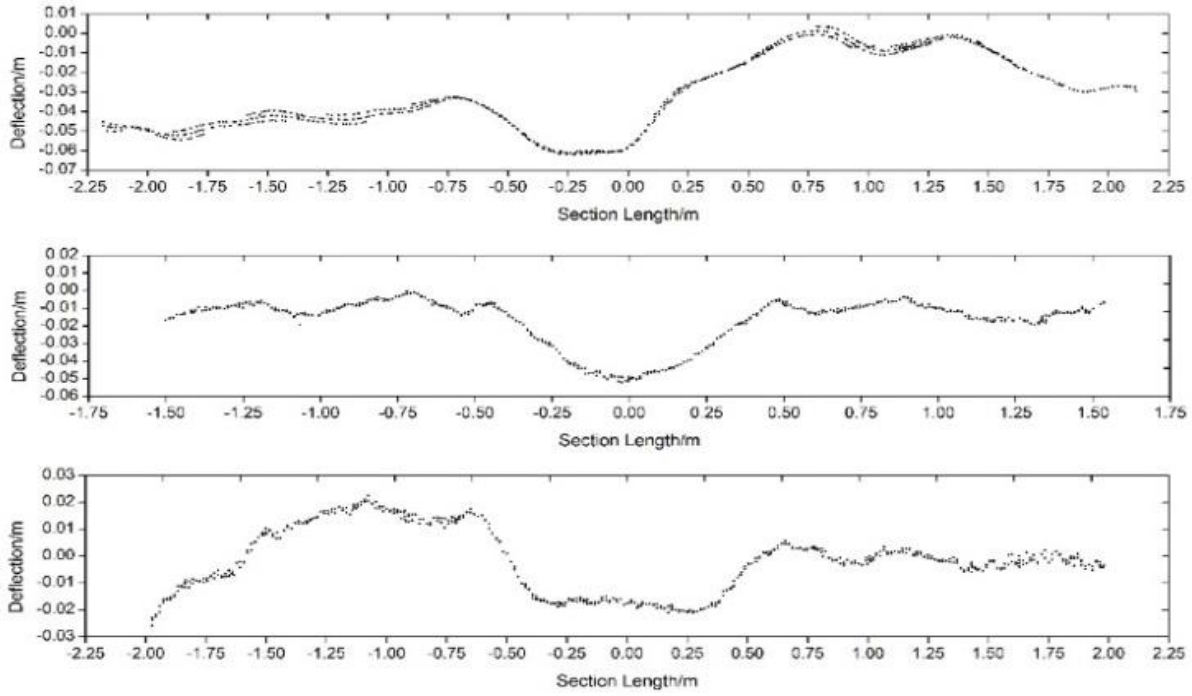

Fig.8. The Distribution of Point Cloud in Sections 1-3

Above characteristic curvature algorithm based on point cloud is used to calculate the characteristic curvature of the point cloud data of three cross sections. The characteristic curvature of the discrete point cloud of cross sections 1-3 is listed in Figure 9.

It can be seen from figure 9 that affected by the noise of point cloud, the damage location of the box girder cannot be judged accurately by the characteristic curvature curve yet. Due to the

outlier noise of the point cloud and the uneven surface of the box girder (as presented in Figure 10), the characteristic curvature algorithm proposed in this paper is also sensitive to the undamaged parts. Consequently, the location of the natural concave convex in the box girder and that of the outlier noise are also identified as the damage location, that is, the trough of the characteristic curvature curve. In this paper, the characteristic curvature algorithm is applied to the identification of the damage location. There are many interference signals in the identified damaged part by the proposed characteristic curvature algorithm, and these interference signals have the characteristics of noise signals, which are characterized by high frequency. However, the low frequency information of the real damage location is masked by the high frequency noise signals. Thus, it is necessary to filter the characteristic curvature curve.

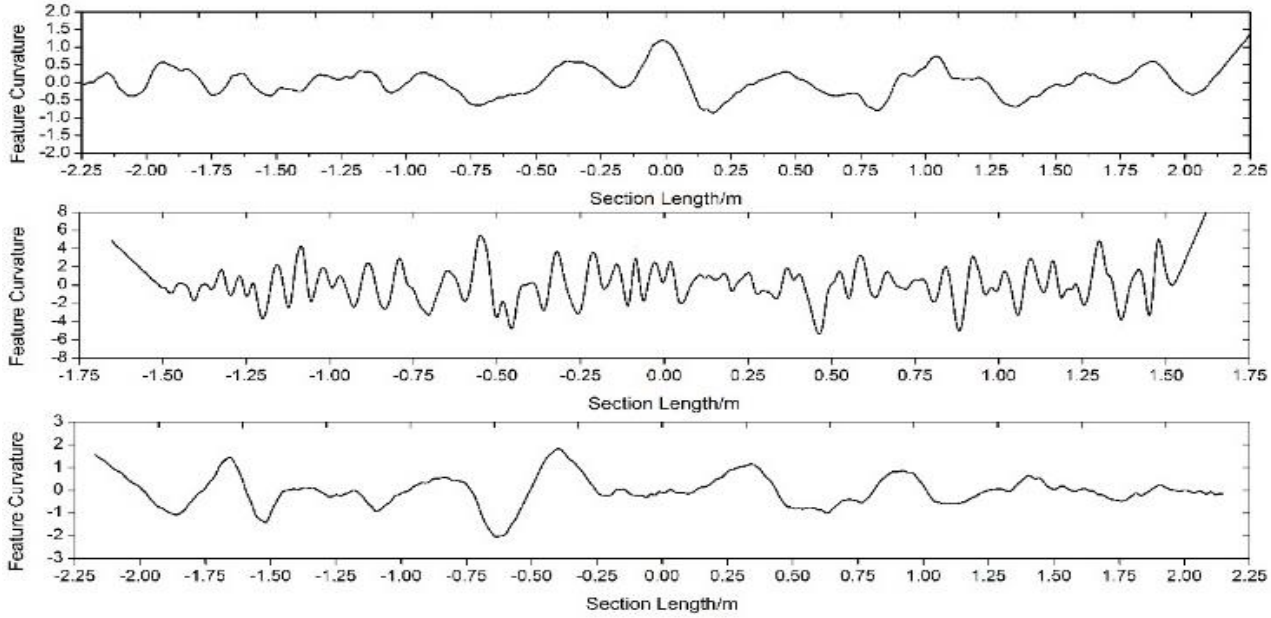

Fig.9. Characteristic Curvature Diagram of Discrete Point Cloud of Sections 1-3

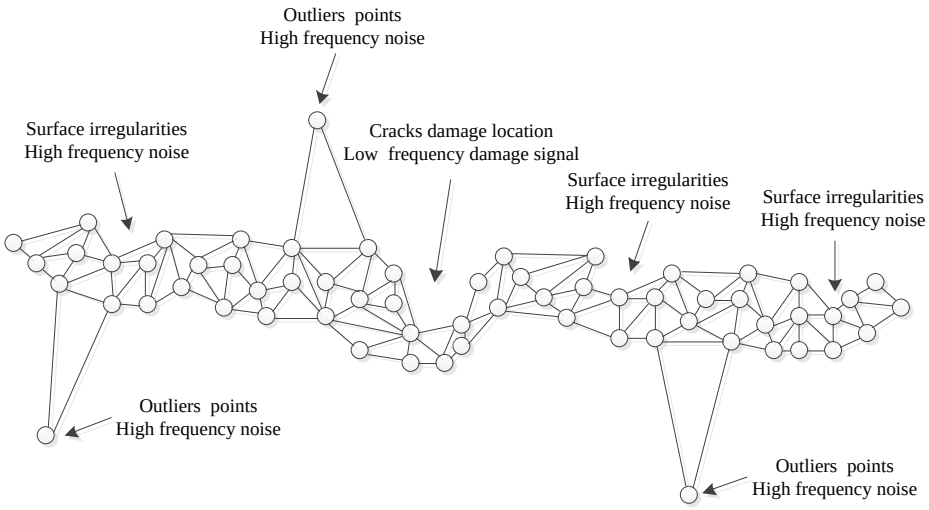

Fig.10. Feature Curvature Signal Constitution Based on Point Cloud

4. Study on Wavelet De-Noising Algorithm Based on Improved Threshold

A finite length signal is assumed as:

$$X(t) = D(t) + \varepsilon(t) \tag{18}$$

In which D(t) is the true signal, ε(t) is the variance of point cloud noise, obeying the distribution of $N(0,\sigma^2)$, t=0, 1, …, N-1, N, and N is the length of the signal. In practice, the useful signal is usually represented by a low frequency signal or a relatively stable signal, and the noise signal is usually represented by a high frequency signal. The principles of wavelet de-noising include: firstly, the signal is decomposed by wavelet transform. Taking the three-layer wavelet as an example, noise is usually included in cd1, cd2 and cd3 as shown in Figure 11; then, the wavelet coefficients after decomposition are processed by thresholding; and finally, the wavelet coefficients after processing are used to reconstruct the signal, by which the purpose of noise removal is achieved.

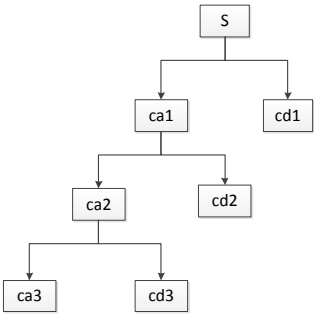

Fig.11. The Structure of Three Layer Wavelet Decomposition

In terms of the conventional threshold de-noising algorithm, there are two kinds of processing methods: hard threshold function and soft threshold function. The hard threshold processing refers to changing the absolute value of the signal that is less than or equal to the threshold to zero, while that is larger than the threshold will not be changed [19]. Its function expression is:

$$\hat{W}_{j,k} = \begin{cases} W_{j,k}, & |W_{j,k}| \geq \lambda \\ 0, & |W_{j,k}| < \lambda \end{cases} \tag{19}$$

Comparatively, the soft threshold processing refers to comparing the absolute value of the signal with the threshold: when the absolute value of the signal is less than or equal to the threshold value, it is zero, while when the data points are larger than the threshold, they are contracted to zero. The value is the difference between the value of the point and the threshold value. Its function expression is:

$$\hat{W}_{j,k} = \begin{cases} sign(W_{j,k})(|W_{j,k}| - \lambda), & |W_{j,k}| \geq \lambda \\ 0, & |W_{j,k}| < \lambda \end{cases}. \tag{20}$$

In this formula, $W_{j,k}$ is the wavelet coefficients after the wavelet transform of noisy signal, λ is the threshold, and is the wavelet coefficients after threshold de-noising. In the hard threshold algorithm, hard threshold function is discontinuous at threshold λ, and additional oscillation is produced by the estimated signal, which is not as smooth as the original signal. By contrast, in the soft threshold algorithm, despite the good overall continuity of wavelet coefficients, the wavelet estimation coefficient after the threshold processing and the wavelet coefficients of each scale before the threshold processing will have a constant deviation when . As a result, the degree of approximation between the reconstructed signal and the original signal will be directly impacted [20-21]. Therefore, it is difficult to effectively filter the high frequency noise signal in the characteristic curvature of the point cloud by conventional threshold de-noising algorithm.

To overcome the shortcomings of the hard threshold and soft threshold methods, an improved noise reduction method is proposed in this paper to solve the problem of high frequency signal in the characteristic curvature based on the point cloud random noise. In this

method, the threshold function is continuous and there is no constant deviation at threshold λ. Meanwhile, the oscillation caused by the hard threshold method can be suppressed and the constant deviation caused by the soft threshold method can be reduced by the wavelet coefficients estimated by this method. Its function expression is:

$$\hat{W}_{j,k} = \begin{cases} W_{j,k} - 0.5\dfrac{\lambda^n \times k}{(W_{j,k})^{n-1}} + (k-1)\lambda, & W_{j,k} > \lambda \\ 0.5\dfrac{|W_{j,k}|^m \times k}{(\lambda)^{m-1}} sign(W_{j,k}), & |W_{j,k}| \le \lambda \\ W_{j,k} + 0.5\dfrac{(\lambda^n) \times k}{(\lambda)^{n-1}} - (k-1)\lambda, & W_{j,k} < -\lambda \end{cases} \tag{21}$$

In the formula, m, n, k refer to the regulators of the improved threshold function, by which the flexibility of the threshold function in practical de-noising applications is enhanced. Moreover, the form of threshold function is determined by parameter, and the value of parameter k is between 0 and 1. If k=0, the improved threshold function is equivalent to the soft threshold function, while if k=1, the improved threshold function is equivalent to the hard threshold function. Therefore, when it is utilized to reduce the noise of high frequency signal in characteristic curvature, the actual application effect can be adjusted by changing the value of parameter k, and the improved threshold function can be made adaptively to select the better de-noising effect. At the same time, the discontinuity of hard threshold function can be avoided, and the constant error in soft threshold function can be reduced. In addition, the improved threshold function has infinite order continuous derivative, which provides the basis for the selection of wavelet adaptive threshold. The improved threshold function is illustrated in figure 12.

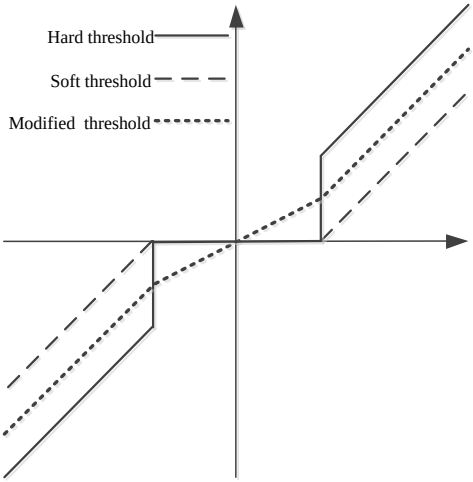

Fig.12. Schematic Diagram of the Improved Threshold Function

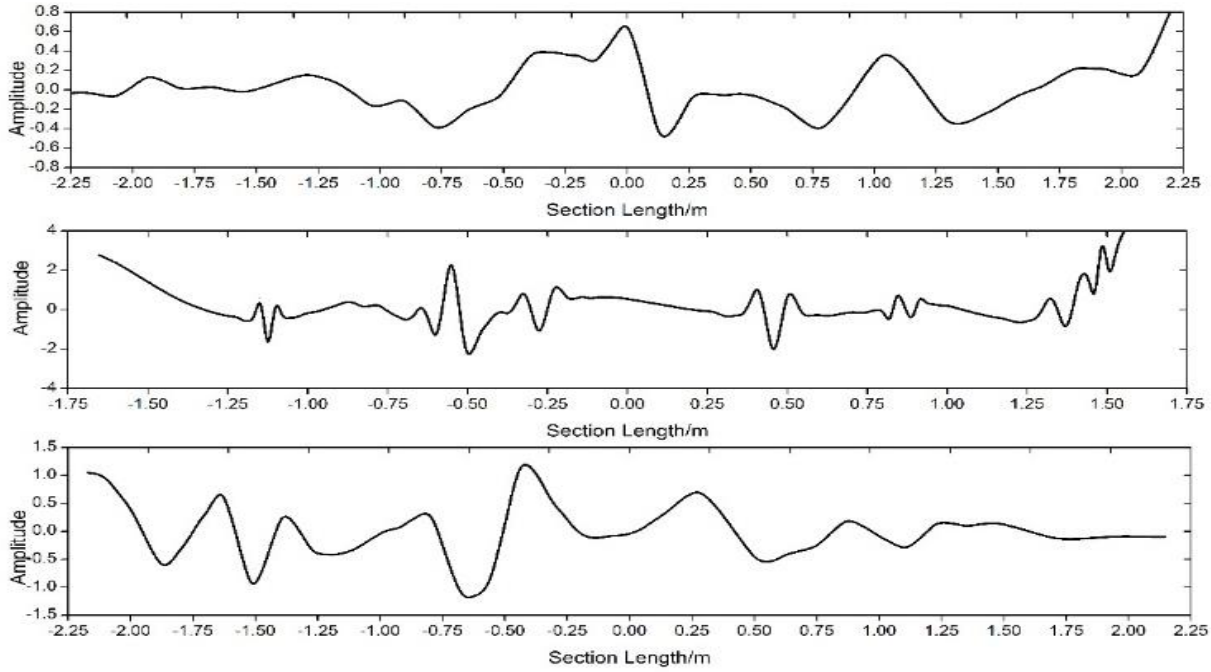

Fig.13. The Characteristic Curvature Map after Processing the Improved Threshold De-noising

The improved threshold de-noising algorithm is used to deal with the characteristic curvature curve in Figure 10, and the characteristic curvature of the cross section after noise reduction is presented in Figure 13. It can be seen from the results that the improved threshold function is used to deal with the noise signal of the characteristic curvature curve, and a better noise reduction effect can be achieved in the condition of keeping a high similarity and energy ratio. Furthermore, the information of high frequency noise can be filtered effectively, and the

characteristic component of the low frequency signal of the damage location can be preserved. Figure 14 exhibits a three-dimensional model of box girder after damage, and the cracks are traced in order to show the distribution of the cracks clearly. Figure 15 displays the corresponding location between the characteristic curvature curve and sections 1-3 of the box girder after the improved threshold de-noising is processed as well as the corresponding position between the damage points of sections 1-3 and the troughs of the characteristic curvature curve

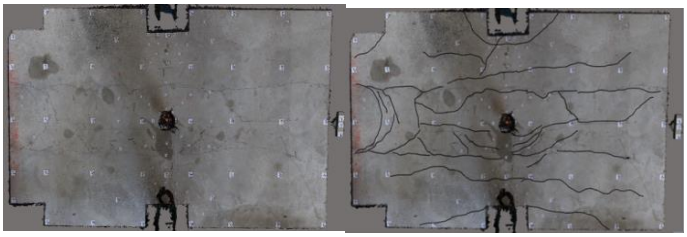

Fig.14. Distribution of Cracks on the Surface of the Box Girder after Loading

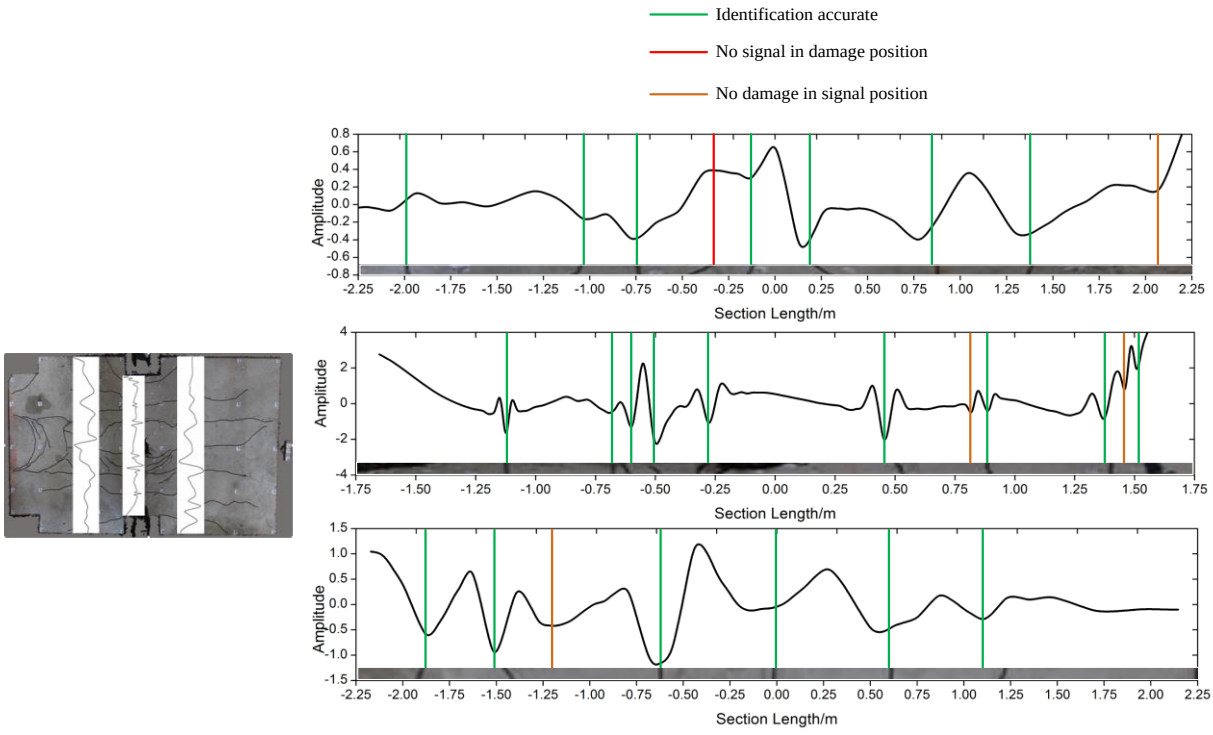

Fig.15. Comparison of the Trough of the Characteristic Curvature Curve and the Corresponding Position of Cross Section Damage

It can be seen that the trough of the characteristic curvature curve after filtering is basically consistent with the crack location of the box girder surface. The characteristic curvature shows obvious changes in the damage location of the box girder, and it can form stable low-frequency

information in 3D reconstruction model of point cloud, which can be identified by the improved wavelet threshold de-noising algorithm proposed in this paper. The accuracy of the proposed method is ideal, and the feasibility of the proposed method based on the characteristic curvature and the improved wavelet threshold de-noising is also verified.

Conclusions

In this paper, a method of damage identification based on the characteristic curvature of point cloud and wavelet threshold de-noising function is proposed. In this method, structural spatial point cloud data acquired by the non-contact measurement technology of SFM are used to identify the damage. Compared with the traditional methods, this method mainly has following improvements:

(1) The relationship between the structural stiffness and the curvature is established by taking advantage of the property that the deflection curvature in any section of the structure has a positive correlation with the stiffness of the beam, and a conclusion is drawn that the curvature of the structural deformation can be used to identify the structural damage. Then, a damage identification method based on SFM and discrete point cloud chord length is presented. In the damage identification process of any cross section in the three dimensional model of box girder, it is found that the untreated characteristic curvature of the point cloud cannot be used to judge the damage location of the box girder accurately by the influence of the point cloud noise and concrete unevenness surface. The wave trough of the characteristic curvature curve is the damage index, and there are many spurious signals in it. Specifically, it seems that the undamaged part also shows some high frequency characteristics on the characteristic curvature curve, while the low frequency information of the real damage location is masked by the high frequency noise signal.

(2) On the basis of correcting the defects of soft and hard threshold functions, an improved wavelet threshold de-noising function is proposed in this paper. The expression changes with the variation in decomposition scale, and it is suitable for the identification and filtering of high frequency noise in point cloud data. Moreover, the noise reduction function can be used to distinguish the abrupt change of the characteristic curvature in damage location and the abnormal high frequency noise signal more effectively. At the same time, the high frequency noise signal can be accurately filtered, and the low frequency signal of damage can be reserved efficiently. More importantly, the expression contains no uncertain parameters, by which the stability of noise reduction can be guaranteed. By using the improved threshold de-noising function in this

paper to deal with the curvature characteristic curve of sections 1-3, the wave trough position of the curve is basically consistent with the damage location. Therefore, the proposed method's effect of damage identification is ideal, and it also has the potential to be applied to actual bridge structural damage identification.

Acknowledgement

This paper was supported by the National Nature Science Foundation of China (NO. 51778094 and No. 51708068).

References

1. D.G. Lowe, Distinctive image features from scale-invariant keypoints, 2004, International Journal of Computer Vision, vol. 60, no. 2, pp. 91-110.
2. I. Gordon, D.G. Lowe, What and where: 3D object recognition with accurate pose, 2006, Toward Category-Level Object Recognition, vol. 4170, pp. 67-82.
3. Y. Furukawa, J. Ponce, Carved visual hulls for image-based modeling, 2009, International Journal of Computer Vision, vol. 81, no. 1, pp.53-67.
4. Y. Furukawa, High-fidelity image-based modeling, 2008, Dissertations & Theses - Gradworks, vol. 12, no. 2, pp. 1825-1860.
5. N. Snavely, S.M. Seitz, R. Szeliski, Modeling the world from internet photo collections, 2008, International Journal of Computer Vision, vol. 80 no. 2, pp. 189-210.
6. M.J. Westoby, J. Brasington, N.F. Glasser, M.J. Hambrey, J.M. Reynolds, 'structure-from-motion' photogrammetry: A low-cost, effective tool for geoscience applications, 2012, Geomorphology, vol. 179, pp. 300-314.
7. S. Harwin, A. Lucieer, Assessing the accuracy of georeferenced point clouds produced via multi-view stereopsis from unmanned aerial vehicle (UAV) imagery, 2012, Remote Sensing, vol. 4, no. 6, pp. 1573-1599.
8. T.N. Tonkin, N.G. Midgley, D.J. Graham, J.C. Labadz, The potential of small unmanned aircraft systems and structure-from-motion for topographic surveys: a test of emerging integrated approaches at cwm idwal, north wales, 2014, Geomorphology, vol. 226, no. 1-2, pp. 35–43.
9. A. Lucieer, D. Turner, D.H. King, S.A. Robinson, Using an unmanned aerial vehicle (UAV) to capture micro-topography of antarctic moss beds, 2013, International Journal of Applied Earth Observation & Geoinformation, vol. 27, no. 4, pp. 53-62.

10. C. Wu, S. Agarwal, B. Curless, S.M. Seitz, Multicore bundle adjustment, 2011, Computer Vision and Pattern Recognition, vol. 42, pp. 3057-3064.
11. K. Wolff, C. Kim, H. Zimmer, C. Schroers, M. Botsch, O. Sorkine-Hornung, Point cloud noise and outlier removal for image-based 3D reconstruction, 2016, Fourth International Conference on 3d Vision, pp. 118-127.
12. D.L. Donoho, De-noising by soft-thresholding, 1995, IEEE Transactions on Information Theory, vol. 41, no. 3, pp. 613-627.
13. S. Sardy, P. Tseng, A. Bruce, Robust wavelet denoising, 2001, IEEE Transactions on Signal Processing, vol. 49, no. 6, pp. 1146-1152.
14. C. Huimin, Z. Ruimei, H. Yanli, Improved threshold denoising method based on wavelet transform, 2012, Physics Procedia, vol. 33, no. 1, pp. 1354-1359.
15. K.N. Snavely, Scene reconstruction and visualization from internet photo collections, 2008, Transactions on Computer Vision & Applications, vol. 3, no. 12, pp. 1909-1911.
16. N. Snavely S.M. Seitz, R. Szeliski, Skeletal graphs for efficient structure from motion, 2008, Computer Vision and Pattern Recognition, vol. 1, pp. 1-8.
17. R. Hartley, Zisserman, A., Multiple view geometry in computer vision, 2001, Kybernetes, vol. 30, no. 9/10, pp. 1865 - 1872.
18. L.M. Shi, F.S. Guo, Z.Y. Hu, An improved PMVS through scene geometric information, 2011, Journal of Automatica Sinica, vol. 37, no. 5, pp. 560-568.
19. E. Güzel, M. Canyilmaz, M. Türk, Application of wavelet-based denoising techniques to remote sensing very low frequency signals, 2016, Radio Science, vol. 46, no. 2, pp. 1-9.
20. X. Dong, S. Mane, Z. Sosic, Characterization of signals, 2015, Electrophoresis, vol. 36, no. 2, pp. 363–370.
21. H. Douzi, D. Mammass, F. Nouboud, Faber-schauder wavelet transform, application to edge detection and image characterization, 2001, Journal of Mathematical Imaging and Vision, vol. 14, no. 2, pp. 91-101.